Journal of Petroleum Science and Technology 12(2): 34, 2022, Pages 17-25
DOI:10.22078/JPST.2023.4840.1808

Journal of Petroleum Science and Technology
Research Paper
https://jpst.ripi.ir/

Comparison of Cementation Factor Determination by Artificial Neural Network Method and Optimized Experimental Relations in Carbonate Rocks

Jafar Vali and Farnusch Hajizadeh*
Department of Mining Engineering, Urmia University, Urmia, Iran

Abstract
The cementation factor is one of the basic parameters for calculating water saturation and then hydrocarbon saturation of reservoirs. The best way to determine the cementation factor is through laboratory measurements. To generalize this coefficient for samples without laboratory measurements, experimental relationships versus petrophysical properties by researchers can be somewhat helpful. The method of artificial neural networks, with the help of training, validation, and data analysis, has given better results in determining the cementation factor of carbonate samples. It is one of the best methods to use petrophysical data as training data and make acceptable predictions with analytical methods. Therefore, laboratory measurement of the cementation factor has been performed for 159 carbonate cores from the Sarvak formation in southwest Iran. For the studied samples, the cementation factor in porosity was determined as a quadratic equation with the highest correlation coefficient. In this study, the compatibility of the experimental relationship shows better conformity by considering the permeability of each sample. Improvement of empirical relationships by the authors, correlation coefficients between the laboratory data, and the experimental relationships have been increased. Therefore, it is better to use improved experimental relationships for the studied carbonate samples. Artificial neural network methods have been used to process the data, best adapt the laboratory data, and present a suitable model. The Bayesian Regularization algorithm with five hidden layers has the least error in the test, validation, and testing stages.

Keywords: Carbonate Rock, Cementation Factor, Artificial Neural Network, Empirical Relationship, Sarvak Formation.

Introduction
Most of the world's crude oil is in the carbonate rocks of the Middle East, and 90% of gas is in these types of rocks [1]. However, carbonate reservoirs are associated with exclusive heterogeneity, and their heterogeneities affect consequent chemical and physical processes, for instance, cementation and compaction [2]. This phenomenon entangles the assignment of reservoir properties because it is essential to oil field development [3].

Laboratory measurements to determine the cementation factor in special core analyses are necessary to determine water saturation. However, the availability of these parameter values is expensive and time-consuming in laboratory measurements. Since water saturation (Sw) is an indispensable parameter in any reservoir evaluation, this factor can be essential in determining water saturation [4]. Although this parameter is of significant importance in determining water saturation in oil and gas reservoirs, there is no compatible and appropriate relationship for the case of Iranian carbonate reservoirs yet [1].

Electrical resistance is an important petrophysical property of reservoir rock. The electrical resistance of a drilling core is measured in the laboratory. Identifying hydrocarbon intervals is determined by using electrical logging data and the electrical resistance of a drilling core in a well. This measurement is also widely used in assessing water saturation in well logging and laboratory studies. Hydrocarbon saturation is calculated indirectly with petrophysical log information and using water saturation formulas [2].

There are two types of conductivity in rocks: electrical conductivity, which is specific to metal sulfides (pyrite, galena, and chalcopyrite), graphite, and metals. Electrolytic conductivity is the result of water with soluble salt in it. In general, the specific resistance of a rock to the specific resistance of water in pores. It depends on the amount of soluble salt, temperature, lithology, percentage of clay in the rock, the type and percentage of conductive minerals, rock texture, and how porosity and conductive minerals are distributed. The solid part of the

**Corresponding author:* Farnusch Haji zadeh, Department of Mining Engineering, Urmia University, Urmia, Iran
E-mail addresses: F.HajiZadeh@urmia.ac.ir
Received 2022-07-19, Received in revised form 2022-11-24, Accepted 2023-01-11, Available online 2023-02-25

rock is the grains, along with the cement between its particles. The conductivity behavior of the solids is possible only due to the abnormal accumulation of large amounts of conductive minerals [5].

Archie (1942) found a correlation between porosity and resistivity formation factor (F). He also used the cementation exponent "m" to describe this empirical correlation that could be useful in formation evaluation studies. Physically, the "m" factor is a measure of the rock's degree of cement and consolidation. Therefore, it is called the cementation factor. In the petrophysical characterization of carbonate reservoirs, the cementation factor is one of the most critical parameters. Its effect on calculating water saturation (Sw), formation resistivity factor, tortuosity (a) of the pore geometry in current flow, and surface area of composite particles is applicable [6]. To calculate the water saturation (Sw) in carbonate reservoirs, the porosity exponent parameter ("m") has to be estimated. The parameter "m" is not a constant, particularly in heterogeneous reservoirs. Its value depends on the porosity type and volume (percentage). Inaccurate estimates of "m" can cause significant errors in calculating water saturation when using Archie's Equation and lead to discrepancies between log interpretation and production examination results [2].

The cementation factor is a complex parameter. It is strongly influenced by the shape of the pore space and the coefficient that converts the total porosity to the effective porosity. The coefficient of cementation depends on factors such as total, effective, secondary porosity, etc. Pores and bottlenecks are pathways for electrical current to pass. Smaller pores are more resistant to conducting electricity than larger throats [7].

The cementation factor increases with increasing pressure. The change in the amount of formation resistance factor against changes in applied pressure depends on the type of porosity and lithology. In moldic porosity, with increasing pressure, the formation resistance factor increases more than in intergranular porosity, which can be due to the closure of small porosities due to pressure in the moldic porosity [8]. Using laboratory parameters of porosity, permeability, and information from petrophysical logs data to determine the empirical relationships coefficient of cementation factor were used. Most of these relationships are related to porosity, and some relationships are related to permeability.

Shel obtained Equation 1 from the study of dolomitic samples to determine the values of "m" in the carbonate medium [9]. In this relation, the cementation factor decreases with an increase in porosity.

$$m = \frac{0.019}{\phi} + 1.87 \quad (1)$$

Nugent (1984) [10] used different well logs to calculate the value of "m". He proposed a formula for the cementation factor in reef formation. He used two neutron and density Logs to calculate total porosity and an acoustic graph to determine effective porosity (As seen in Equation 2).

$$m = \frac{2\log\phi_s}{\log\phi_t} \quad (2)$$

In this relation, Φ_s is the porosity of the acoustic graph, and Φ_t is the total porosity.

Borai [11] found that Shel's formula is not applicable for porosity less than 10% in carbonate rocks. In order to improve the Shel relation [9], Equation 3 is presented. In this relation, increasing the porosity, the cementation factor also increases.

$$m = 2.02 - \frac{0.035}{\phi + 0.042} \quad (3)$$

Asquith (1985) [12] introduced a new formula by changing the Nugent (1984) model. In distinguishing between moldic porosity and vuggy porosity in the model Nugent (1984) presented, Equation 4 was used for core samples with moldic porosity.

$$\varphi_{vug} = 2(\varphi_t - \varphi_s)\varphi_m = \varphi_t - 2(\varphi_t - \varphi_s)m \geq \frac{(2\log\varphi_m)}{(\log\varphi_t)} \quad (4)$$

In this relation, "m" is the cementation factor, Φ_m is the moldic porosity, Φ_{vug} is the vuggy porosity, and Φ_t is the total porosity. In Equation 5, the experimental relation between the cementation factor and porosity by Sethi (1979) is shown [13]:

$$m = 2.05 + \phi \quad (5)$$

Fuk-Mann (1987) showed that the cementation factor is related to the rock type and permeability in addition to the amount of porosity, and presented the following formulas based on the range of permeability in carbonate rocks (as seen in Equation 6).

$$\begin{aligned} &A: \quad m = 1.2 + 0.128\Phi (k < 0.1 mD) \\ &B: \quad m = 1.4 + 0.0857\Phi (0.1 < k < 1 mD) \\ &C: \quad m = 1.2 + 0.0829\Phi (1.0 < k < 100\ mD) \\ &D: \quad m = 1.22 + 0.034\Phi (k > 100 mD) \end{aligned} \quad (6)$$

As seen in all the empirical relationships of other researchers, the value of "m" is predicted in terms of porosity. Only in the Focke-Mann (1987) [8] predicted by Φ and different ranges of permeability values.

In all experimental relationships presented in this study, except for the experimental relationship of Shel (1984) [9], the cementation factor of the samples increases by increasing the amount of porosity. It is also observed in the studied samples.

New experimental relationships and finding the best agreement between laboratory measurement data and empirical relationships have been done. Also, the amount of Cementation factor has been calculated from an artificial neural network method using porosity and permeability data of each sample.

The amount of cementation factor is predicted based on the petrophysical data of the drilling core, including porosity and permeability in the method of artificial neural networks using various algorithms, including Levenberg Marquardt, Bayesian regularization, and Scaled conjugate Gradient. The results show that the amount of cementation factor using the Bayesian regularization algorithm has the best agreement with the laboratory results with the least error.

Therefore, having a limited number of laboratory data and presenting a suitable algorithm in the artificial neural network method, the amount of cementation factor can be predicted for the whole formation.

Geological Description of Sarvak Formation

The Sarvak formation is one of the formations of the

Bangestan group. Due to its hydrocarbon reservoir potential, this formation is considered one of the essential strata units in the Zagros basin [14]. Sarvak formation is in the stratigraphic units of the Bangestan group and the middle cretaceous age. The average thickness of the reservoir is between 55 to 73 meters. Sarvak formation is under various diagenetic events such as dissolution and dolomitization, which affects the porosity and permeability of the reservoir, consequently, the rate of production [15]. In this study, for some selected samples, a thin section was studied to determine the porosity type. Therefore, XRD results for mineralogy, SEM images to show the pore types, and the pore throat size distribution of the studied cores from MICP are suitable.

Materials and Methods

Materials

Thin Section Study

The optical observation was performed using transmitted light microscopy for fifty-eight carbonate samples (30-micron thick samples). In addition, lithotypes were studied after impregnating the samples with blue epoxy resin using a professional geological microscope [16,17]. The thin section analysis of selected samples shows that porosity types of samples are Inter Particle and Visual porosity, Inter Particle and Vuggy Visual porosity, Vuggy Visual porosity, and Intercrystaline and Vuggy Visual Porosity.

Artificial Neural Network

An Artificial Neural Network (ANN) is a popular statistical method. That explores the relationships between variables with high accuracy [18-21]. Essentially, the structure of an ANN is computer-based. That consists of several simple processing elements operating in parallel [20, 22, 23]. An ANN consists of input, hidden, and output layers. Hence, it is referred to as a three-layer network. The input layer contains independent variables connected to the hidden layer for processing. The hidden layer contains activation functions and calculates the variables' weights. It explores the effects of predictors on the target (dependent) variables. Finally, in the output layer, the prediction or classification process is ended. The results are presented with a small estimation error [24,25].

Recent examples include permeability prediction with ANNs from well logs data, generation of synthetic wireline logs from other logs [26, 27], identification of lithological and depositional facies via a competitive neural network [28, 29], and fuzzy logic [30]. It also includes the estimation of reservoir permeability using an integration of the genetic algorithm and a coactive neuro-fuzzy inference system [31]. Due to the convergence speed of the Levenberg – Marquardt, Bayesian Regularization, and Scaled Conjugate Gradient algorithms in the leading networks, these algorithms have been used to train the target network, and the parameters errors have been used to evaluate the performance of the model. Appropriate network training is vitally important to give better performance [32].

Model Evaluation Criteria

To compare the performance of the models, the mean square error (MSE), the root mean square error (RMSE), the Geometric Mean Error Ratio (GMER), and the mean absolute percentage error (MAPE) parameters have been used, which it can be calculated from the following relations.

$$MSE=\frac{\sum_{i=1}^{j}(O_i-P_i)^2}{j} \quad (7)$$

$$RMSE=\sqrt{\frac{\sum_{i=1}^{j}(O_i-P_i)^2}{j}} \quad (8)$$

$$GMER=\exp\left[\frac{1}{j}\sum_{i=1}^{j}\ln\left(\frac{P_i}{O_i}\right)\right] \quad (9)$$

$$MAPE=\frac{\sum_{i=1}^{j}\left|\frac{Oi-Pi}{Oi}\right|}{j}*100\% \quad (10)$$

where j is the total number of observations Oi and prediction Pi, respectively, RMSE values are not negative and vary from zero to infinity. Low RMSE values indicate the high accuracy of the model. The GMER parameter indicates the consistency between the observed and predicted values. If the value of the GMER is equal to one, there is a perfect match between the measured and the predicted values. On the other hand, more or less of this parameter indicates the overestimation or underestimation of the model, respectively [33].

Methods

Two methods have been used to determine Archie's coefficient in the laboratory. In the first method (Archie's method), by assuming *a*=1 in algebraic form, the formation resistivity factor is inversely proportional to porosity where the slope of the line is "m" the cementation exponent.

When Archie's curve cannot cross the given points, in this situation, a curve is drawn that has the best fitting compared to the other points. The location where this line intercepts the logarithmic-logarithmic graph (FRF and Φ), in porosity of 100%, then the value of FRF at the intercept (a), is found by 'free' regression. If "a" is not equal to 1, then this implies that Ro at 100% porosity is not equal to Rw, the value of is shown. In other words, the interpretation of "m" when Archi's curve fails to fit the points best. In this case, *a*=1 is presumed, and "m" is a function of porosity. Different values of "m" with porosity were reported [34].

From one of the oil fields in southwest Iran, 159 carbonate plug samples were selected. To conduct the tests, initially, samples are cleaned in a Soxhlet system to remove crude oil, brine, drilling mud, or any other fluid within the pores. Then, the samples are left in a conventional oven until they are completely dried. The porosity and specific gravity of the sample were measured by Ultra-Porosimeter. Knowing the total volume and mass of the sample, the porosity values and specific gravity of the rock were calculated. Ultra-Permeameter apparatus was used to measure absolute gas permeability [35].

To measure the formation resistivity factor, samples are saturated by formation brine, and the sample pore volume is calculated from gravimetric measurements before and after saturation.

brine resistivity (Rw) and resistivity of the plug sample (Ro) saturated with brine are measured. An Overburden FRF Rig device has been used to measure the specific resistance of saturated samples of the formation brine. The sample is placed in the core holder under the reservoir pressure conditions. After reaching the equilibrium conditions, the sample's electrical resistance value by using the HIOKI-LCR resistor device is measured versus ohmic [36].

The tests are performed using a two-electrode hydrostatic overburden core holder capable of operating at the specified maximum test stress. Resistance (r) of the sample was measured along the longitudinal axis in reservoir pressure conditions. Afterward, the special resistance of the water-saturated sample (Ro) is calculated from the physical dimension of the sample (A and L). The formation resistivity factor (F) was obtained as a ratio of brine-saturated rock resistivity (Ro) to formation brine resistivity (Rw).

$$F=\frac{R_o}{R_w}=\frac{a}{\varphi^m} \quad \text{or } \mathrm{Log}(F)=\mathrm{Log}(a)-m\log(\varphi) \qquad (11)$$

"m" is the slope of the best-fit regression to the plotted points, while the tortuosity factor "a" is the line intercept at φ =1. The equation implies that a beaker of saturation fluid (that is φ =1) has a resistivity of Ro = a × Rw, which is obviously in error. To overcome this problem, the constant "a" is fixed on 1. [37].

The permeability of one sample is less than 0.1 mD, thirty-nine samples are 0.1 to 1 mD, One hundred four samples are 1 to 100 mD, and eleven samples are more than 100 mD. The cementation factor of the samples is in the range of 1.59 to 3.96. The main steps of the methodology are illustrated in Figure 1. In this Figure, the work method includes laboratory measurements of the cementation factor, determining its value using the researchers' experimental relationships, as well as its prediction in terms of petrophysical properties using ANN for the studied samples, which are presented as a flowchart. The reliability of the technique is verified by applying the samples from carbonate reservoir rocks (as shown in Figure 1).

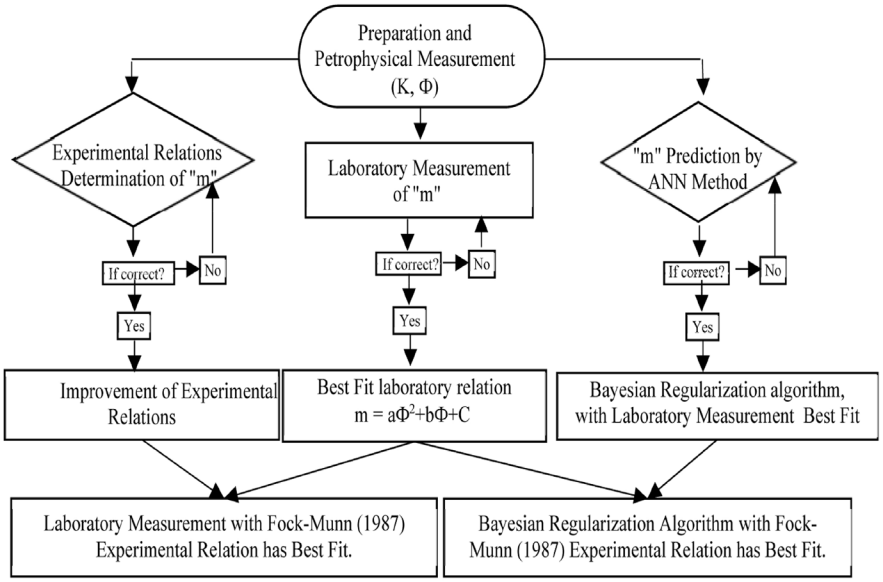

Fig. 1 Proposed methodology flowchart.

To present a new method that can better predict the amount of cementation factor in this wide range of porosity and permeability data, the artificial neural network method can be used In this study, Levenberg Marquardt, Bayesian Regularization, and Gradient Scaled Conjugate algorithms have been used to predict the amount of cementation factor versus petrophysical properties to compare algorithms.

Results and Discussion

The main steps of the studied methodology include determining the cementation factor by using laboratory measurements, the researchers' experimental relationships, and prediction by ANN, presented in Figure 1. For the studied samples, the cementation factor in terms of porosity as a quadratic equation $m = a\phi^2 + b\phi + c$ has the highest correlation coefficient (0.82), which shows the relationship between the cementation factor resulting from the Archi relation and the porosity of the drilling core (as seen in Figure 2). Also, in this study, the type of porosity was determined by using a thin section study, and this study shows that for some selected samples with a cementation factor is three and above, the type of porosity is inter particles and vuggy visual porosity.

As shown in Table 1, the correlation coefficients between the laboratory data and the experimental relationships of Shel (1984), Sethi (1979), Borai (1985), and Fock-Munn (1987) are 45, 78, 56, and 78, respectively. However, with the improvement of empirical relationships by the authors, the correlation coefficient values have been increased to 78, 79, 62, and 83, respectively. Therefore, using these improved experimental relationships for the studied carbonate samples is better. A comparison of laboratory values of the cementation factor and values obtained from the studied experimental relationships is shown in Figure 3. In this study, the experimental data of carbonate samples show the best agreement and the highest correlation coefficient with Fock-Munn's experimental relationship (1987) in Figure 4.

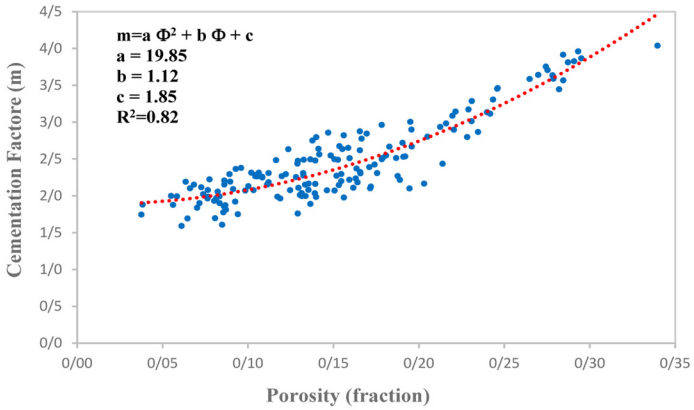

Fig. 2 Cementation factor obtained from Archie relation versus porosity of samples with the highest correlation coefficient in the quadratic equation.

Table 1 Improved cementation factor relationships versus porosity in experimental relationships of Shel (1984), Sethi (1979), Borai (1985), and Fock-Munn (1987).

Presenter	Primary empirical relationship	correlation coefficient	Improved empirical relationship by the authors	correlation coefficient after Improved
Shel (1984)	$m=\frac{0.019}{\phi}+1.87$	45	$m=\frac{2.05\times\phi}{100}+1.90$	78
(1979) Sethi	$m=2.05+\phi$	78	$m=2.40+\phi$	79
Borai (1985)	$m=2.02-\frac{0.035}{\phi+0.042}$	56	$m=2.7-\frac{0.035}{\phi+1}$	62
Fock – Munn (1987)	$m=1.2+0.128\Phi(k<0.1mD)$ $m=1.4+0.0857\Phi(0.1<k<1mD)$ $m=1.2+0.0829\Phi(1.0<k<100\ mD)$ $m=1.22+0.034\Phi(k>100mD)$	78	$m=1.2+0.128\frac{\Phi}{2}(k<0.1mD)$ $m=1.3+0.0857\Phi(0.1<k<1mD)$ $m=1+0.0829\Phi(1.0<k<100\ mD)$ $m=1.4+0.034\Phi(k>100mD)$	83

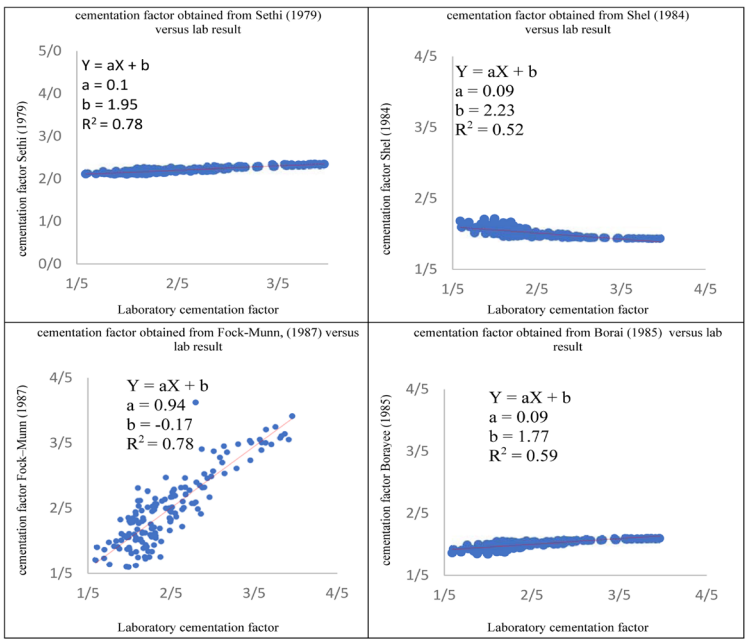

Fig. 3 Comparison of laboratory cementation factor and experimental relations, Sell (1984), Sethi (1979), Borai (1985), and Fock-Munn (1987).

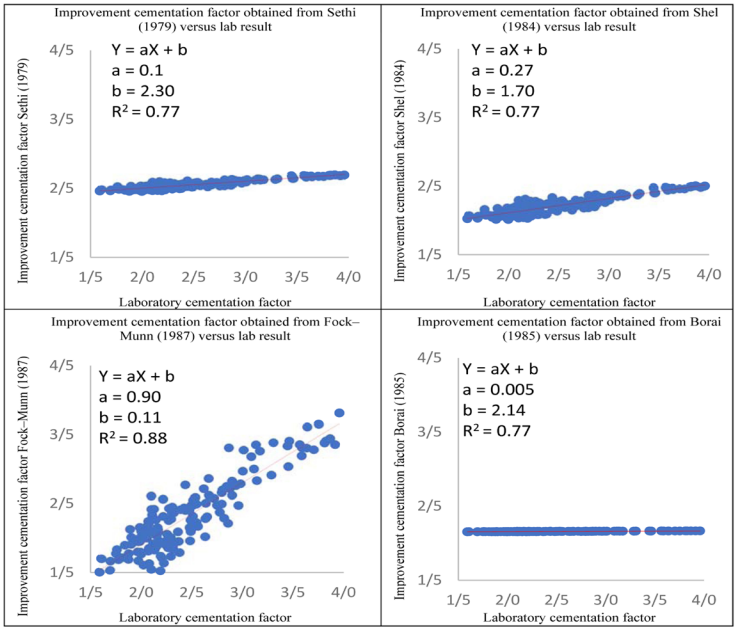

Fig. 4 Comparison of laboratory cementation factor and Improvement experimental relations, Shel (1984), Sethi (1979), Borai (1985) and Fock-Munn (1987), Improvement cementation factor by using Fock–Munn (1987) model is the best fit to laboratory cementation factor values.

The artificial neural network method has been used to predict the cementation factor more accurately. In this study, 98 samples (65%) in the training process, 30 samples (20%) in the validation process, and 23 samples (15%) in the test process are used. The amount of MSE error in each process is calculated from the algorithms. In addition, the error values of RMSE, GMER, and MAPE are computed in each algorithm. Finally, all results for comparison are given in Table 2.

In this study, using different algorithms in artificial neural network methods such as Levenberg - Marquardt, Bayesian Regularization, and Scaled Conjugate Gradient for selected samples, the amount of cementation factor in terms of porosity and permeability was evaluated and predicted. Validation and testing for all three algorithms were compared with the input data. The Bayesian Regularization algorithm with 5 hidden layers has the least error compared to the input data (Table 2 and Figure 5).

Table 2 The amount of error in different algorithms by using 5 and 10 hidden layers in artificial neural network method to determine the coefficient of cementation factor versus porosity and permeability, Bayesian Regularization algorithm with five hidden layers has the lowest error, Average laboratory measurement of cementation factor is 2.47.

Algorithm:	Levenberg - Marquardt		Bayesian Regularization		Scaled Conjugate Gradient	
The number of Hidden Layers:	Ten Hidden Layer	Five Hidden Layer	Ten Hidden Layer	Five Hidden Layer	Ten Hidden Layer	Five Hidden Layer
Average Cementation Factor	2.48	2.41	2.45	2.47	2.48	2.48
MSE	0.007	0.012	0.007	0.006	0.005	0.007
RMSE	0.081	0.110	0.086	0.076	0.070	0.081
GMER	1.027	1.028	1.028	1.022	1.024	1.027
MAPE	2.709	2.727	2.788	2.176	2.362	2.709

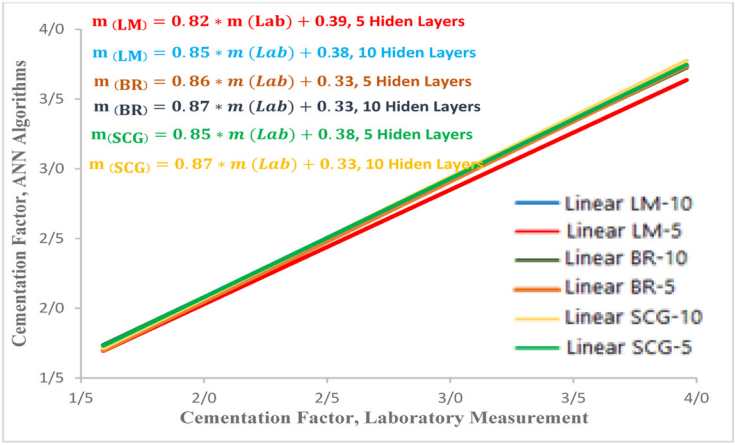

Fig. 5 Diagram of predicted cementation factor versus laboratory measurement in the Levenberg – Marquardt (LM), Bayesian Regularization (BR), and Scaled Conjugate Gradient algorithms (SCG). Bayesian Regularization has the best fit by laboratory measurement.

The results show that this model is highly capable of estimating the cementation factor in the experimental stage using a set of porosity and permeability input parameters and can be used for studies with similar conditions. Furthermore, using the artificial neural network method, the cementation factor can be predicted with higher accuracy than the experimental relationships presented. Moreover, the relationship between input data (porosity and permeability) and the values of the cementation factor resulting from laboratory measurements are validated. Therefore, with a minimum error, the cementation factor can be predicted for other samples in the study formation (Figure 6).

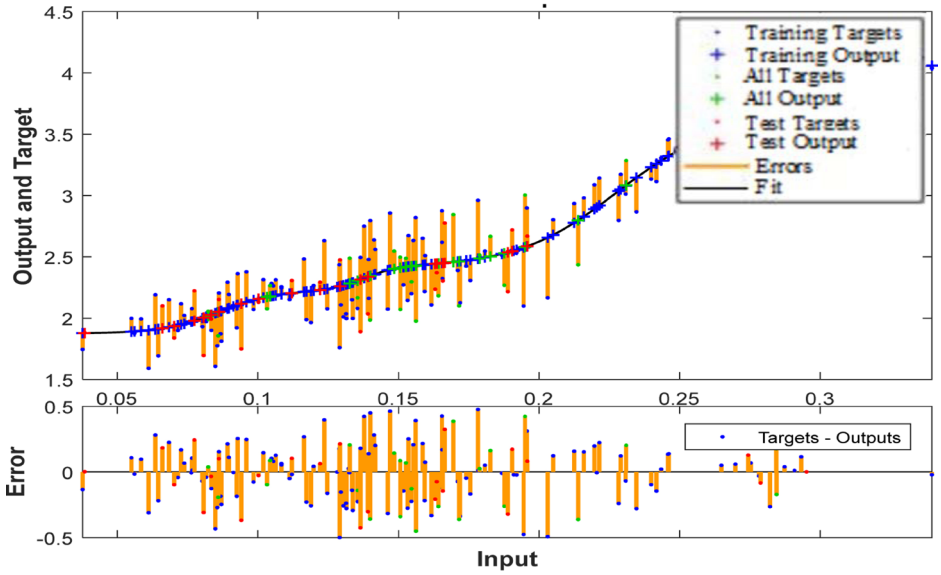

Fig. 6 Target and Errors in prediction parameters in Bayesian Regularization (BR) algorithm by 5 hidden layers.

Cementation factor predicted by the ANN method and Bayesian Regularization algorithm, this model compared with experimental relations such as Shel (1984), Sethi (1979), Borai (1985), and Fock-Munn (1987) shoes in Figure 7. In this figure, the experimental relation Fock-Munn (1987), is more evident compatibility with the Bayesian Regularization algorithm.

Figure 8 compares the improvement experimental cementation factor by the Fock – Munn (1987) model versus the one predicted by the ANN method and Bayesian Regularization algorithm in different air permeability rang. Moreover, Carbonate samples with a permeability range of 0.1 to 1 mD have the most agreement with each other.

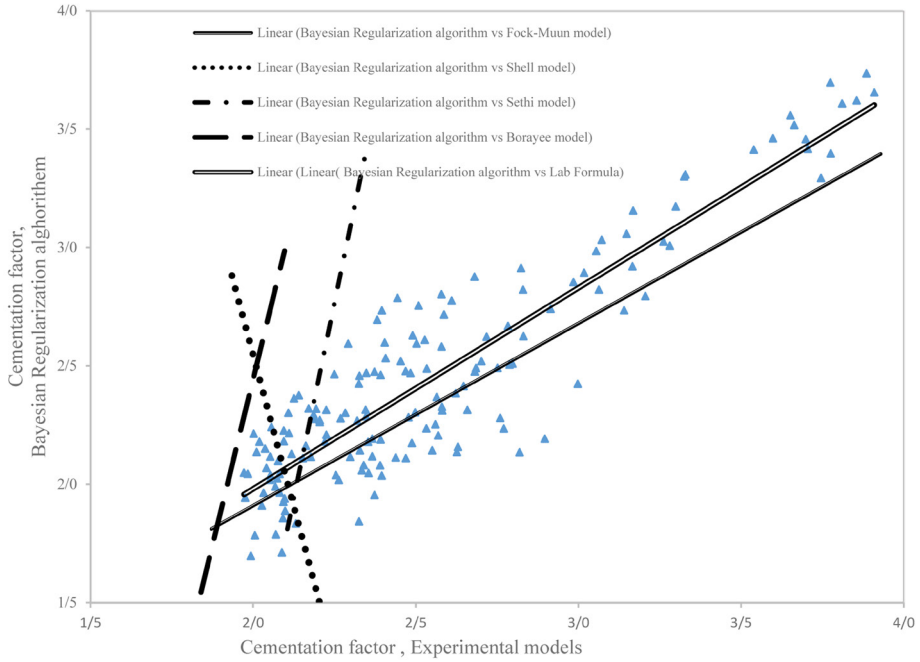

Fig. 7 Cementation factor, ANN method - Bayesian Regularization algorithm versus Lab experimental formula and Shel (1984), Sethi (1979), Borai (1985) and Fock-Munn (1987) relations, Fock-Munn (1987) model compatibility is evident by the Bayesian Regularization algorithm.

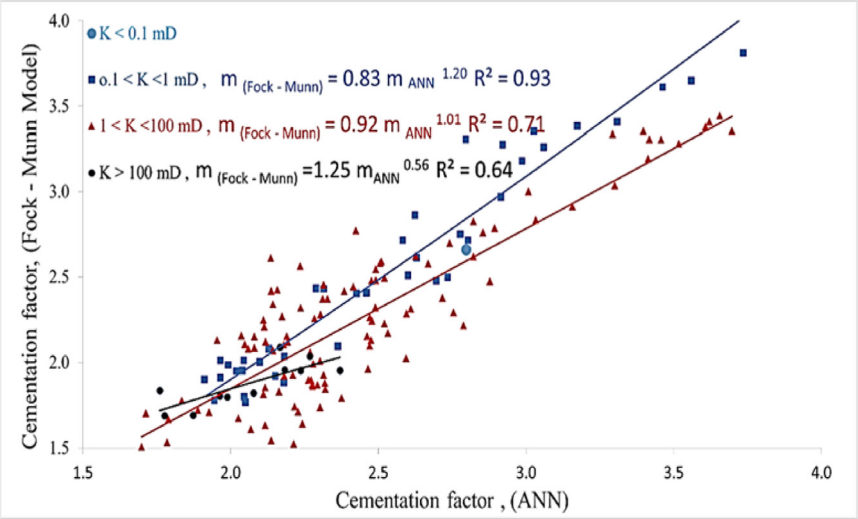

Fig. 8 Improvement experimental cementation factor by Fock – Munn (1987) model versus cementation factor predicted by ANN method and Bayesian Regularization algorithm in different air permeability rang.

Conclusions

The following remarks and conclusions are achieved from this study:

1. For the carbonate samples in Sarvak formation, the experimental relation of the cementation factor in terms of porosity as a quadratic equation $m = a\phi^2 + b\phi + c$ has the highest correlation coefficient.
2. Improvement of empirical relationships by the authors, Correlation coefficients between the laboratory data, and the experimental relationships of Shel (1984), Sethi (1979), Borai (1985), and Fock-Munn (1987) has been increased. Therefore, it is better to use improved experimental relationships for the studied carbonate samples.
3. Comparison of laboratory values of cementation factor and values obtained from the studied experimental relationships show the best agreement and the highest correlation coefficient in different ranges of permeability with Fock-Munn's (1987) experimental model.
4. The amount of cementation factor by the artificial neural network method in terms of porosity and permeability was evaluated and predicted. Compared to other algorithms, the Bayesian Regularization algorithm with five hidden layers has the least error compared to the input data.
5. The cementation factor using the ANN method can be predicted with higher accuracy than the experimental relationships. Therefore, with a minimum error, the cementation factor can be used in the ANN method for other samples in this formation.
6. The Bayesian Regularization algorithm versus other experimental relations only shows good compatibility with the Fock-Munn (1987) model.
7. Comparing the improved cementation factor by the Fock – Munn (1987) model with the one predicted by the Bayesian Regularization algorithm in different air permeability ranges shows that carbonate samples with a permeability of 0.1 to 1 mD have the highest agreement with each other.

Parameters

ANN, Artificial Neural Network.
a, Constant in Archi's Equation.
BR, Bayesian Regularization Algorithm.
F or FF or FRF, The Constant of Proportionality is Termed the Formation Resistivity Factor or Formation Factor.
GMER, Geometric Mean Error Ratio.
K, Permeability.
LM, Levenberg – Marquardt Algorithm.
m, Cementation Factor.
MAPE, Mean Absolute Percentage Error.
MICP, Mercury Injection Capillary Pressure.
MSE, Mean Square Error.
RMSE, Root Mean Square Error.
Rw, Formation Brine Resistivity.
Ro Water-Saturated Rock Resistivity.
SCG, Scaled Conjugate Gradient Algorithms.
SEM, Scanning Electron Microscope.
XRD, X-Ray Diffraction.
Greek letters
Φ, Porosity.
Φ_m, Mold Porosity.
Φ_{vug}, Vuggy Porosity.
Φ_t, Total Porosity.
Φ_s, Porosity of the Acoustic Graph.
Subscripts
A, Cross Section, m^2
L, Sample Length, m.

References

1. Mahmoodpour S, Kamari E, Esfahani M R, Karimi MehrA (2020) Prediction of cementation factor for low-permeability iranian carbonate reservoirs using particle swarm optimization-artificial neural network model and genetic programming algorithm, Journal of Petroleum Science and Engineering, S0920-4105, 20: 31156-6.
2. Archie G E (1942) The electrical resistivity logs an aid in determining some reservoir characteristics, PetroleumTechnology, 5: 32-37.
3. Jodry R L, (1992) Pore geometry of carbonate rocks and capillary pressure curves (basic geologic concepts), Developments in Petroleum Science, Elsevier. 30: 331-377.

4. Liu X p, Hu X-X (2012) Effects of pore structure to electrical properties in tight gas reservoirs: an experimental study, SPE 150926, Austria.
5. Keller G V, Frischknecht F C (1966) Electrical methods in geophysical prospecting, pergamon press, Oxford.
6. Pulido H, Samaniego F, Galicia-Muñoz G, Rivera J, Vélez C (2007) Petrophysical characterization of carbonate naturally fractured reservoir for use in dual porosity simulator, Proceeding, Thirty-Second Workshop on Geothermal Reservoir Engineering, Stanford University, Stanford, California, SGP-TR-183.
7. Winsauer W O, Shearin Jr, H M, Masson P Y, Williams M (1952) Resistivity of brine-saturated sands in relation to pore geometry, AAPG bulletin, 36, 2: 253-277.
8. Focke J W, Munn D (1987) Cementation exponents (m) in Middle Eastern carbonate reservoirs, SPE Formation Evaluation, 2, 02, 155-167, doi.org/10.2118/13735-PA.
9. Schlumberger log interpretation charts (2009) 1020 edition, Shel Company, 1-292.
10. Nugent W H, Brie A, Johnson D L, Nurmi R D (1985) Effect of spherical pores on acoustic and resistivity measurements, presented at the Soc. of Professional Well Log Analysts 26th Annual Logging Symposium, Dallas, Texas.
11. Borai A.M., (1984) A new correlation for cementation factor in low-porosity carbonates, SPE 14401, 22-25: 1985.
12. Asquith G B (1985) Handbook of log evaluation techniques for carbonate reservoirs, Association of Petroleum Geologists, 5.
13. Sethi D K (1979) Some considerations about the formation resistivity factor-porosity relations, 20th SPWLA Symposium.
14. Motiei H (1993) Stratigraphy of Zagros, Geological Survey of Iran Publication, Tehran, 536.
15. Masoudi P, Tokhmechi B, Bashari A, Jafari M A (2012) Identifying productive zones of the Sarvak formation by integrating outputs of different classification methods, Journal of Geophysics and Engineering, 9, 3: 282-290.
16. Lucia F J (1983) Petrophysical parameters estimated from visual descriptions of carbonate rocks: a field classification of carbonate pore space, Journal of Petroleum Technology, 35: 629-637.
17. Dunham R J, Ham W E (1962) Classification of Carbonate Rocks According to Depositional Texture1, in Classification of Carbonate Rocks—A Symposium, 1, ed: American Association of Petroleum Geologists, 0.
18. Alaniz A Y, Sanchez E N, Loukianov A G (2007) Discrete-time adaptive back stepping nonlinear control via high-order neural networks, IEEE Transactions on Neural Networks, 18: 1185–1195.
19. Khomfoi S, Tolbert L M (2007) Fault diagnostic system for a multilevel inverter using a neural network, IEEE Trans Power Electron, 22: 1062–1069.
20. Okut H, Gianola D, Rosa G J M (2011) Weigel K A. Prediction of body mass index in mice using dense molecular markers and a regularized neural network, Genetics Research, 93: 189–201.
21. Vigdor B, Lerner B (2006) Accurate and fast off and online fuzzy ARTMAP-based image classification with application to genetic abnormality diagnosis, IEEE Transactions on Neural Networks, 17: 1288–1300.
22. Gianola D, Okut H, Weigel K A, Rosa G J M (2011) Predicting complex quantitative traits with Bayesian neural networks, A Case Study with Jersey Cows and Wheat, BMC Genet, 12: 1–37.
23. Moller F M (1993) A scaled conjugate gradient algorithm for fast supervised learning, Neural networks, 6, 4: 525–533,doi.org/10.1016/S0893-6080(05)80056-5.
24. Hagan M T, Menhaj M B (1994) Training feedforward networks with the Marquardt algorithm, IEEE transactions on Neural Networks, 5: 989–993.
25. Saini L M (2008) Peak load forecasting using Bayesian regularization, Resilient and adaptive backpropagation learning based artificial neural networks, Electric Power Systems Research, 78, 7: 1302-1310.
26. Mohaghegh S, Arefi R, Ameri S, Hefner M H (1994) A methodology approach for reservoir heterogeneity characterization using artificial neural networks, SPE Annual Technical Conference and Exhibition, 25–28 September, New Orleans, Louisiana, SPE-28394- MS.
27. Shokir E M, El-MAlsughayer A A, Al-Ateeq A (2006) Permeability estimation from well logging responses, Canadian International Petroleum Conference, 7–9 June, Calgary, Alberta, PETSOC-2005-012.
28. Wong P, Amnizadeh F, Nikravesh M (2002) Soft computing for reservoir characterization and modelling soft computing and earth science, Springer-Verlag, Berlin.
29. Rezaee R M, Kadkhaodaie-Ilkhchi A, Alizadeh M P (2007) Intelligent approaches for the synthesis of petrophysical logs, Journal of Geophysics and Engineering, 5, 1: 12–26.
30. Saggaf M.M, Nebrija E L (2003) A fuzzy logic approach for the estimation of lithologies and depositional facies from wireline logs, AAPG Bulletin, 87, 7: 1223–1240.
31. Saemi M, Ahmadi M (2008) Integration of genetic and a coactive neuro-fuzzy inference system for permeability prediction from well logs data, Transport in Porous Media, 71, 3: 273–288.
32. García-Pedrajas N, Hervás-Martínez C, Muñoz-Pérez J (2003) Covnet: a cooperative coevolutionary model for evolving artificial neural networks, IEEE Transactions on Neural Networks, 14, 3: 575-596.
33. Gujarati D N (2004) Multiple regression analysis: The problem of inference, Basic Econometrics, Chapter 8, 264.
34. Perez - Rosale C (1982) On the relationship between formation resistivity factor and porosity, SPE, 531-536.
35. https://www.corelab.com/cli/routine-rock/soxhlet-extraction-apparatus,cli/university-training/porosimeter-porg-200 and cli/routine-rock/ultra-perm gas-permeameter
36. https://ripi.ir/services-and-products/research-and-consulting-services/287-2014-05-18-11-16-44, Determination of cementation coefficient (m) and constant value of a sample of reservoir rock plug up to 4 different pressures, 950-1-18.
37. McPhee C, Reed J, Zubizarreta I (2015) Core Analysis, A Best Practice Guide, Elsevier Science.